Charm annihilation effects on the hyperfine splitting in charmonium

L. Levkova and C. DeTar

Charm annihilation effects on the hyperfine splitting in charmonium

L. Levkova[1] and C. DeTar[1]

[1]*Physics Department, University of Utah, Salt Lake City, UT 84112, USA*

Abstract

In calculations of the hyperfine splitting in charmonium, the contributions of the disconnected diagrams are considered small and are typically ignored. We aim to estimate nonperturbatively the size of the resulting correction, which may eventually be needed in high precision calculations of the charmonium spectrum. We study this problem in the quenched and unquenched QCD cases. On dynamical ensembles the disconnected charmonium propagators contain light modes which complicate the extraction of the signal at large distances. In the fully quenched case, where there are no such light modes, the interpretation of the signal is simplified. We present results from lattices with $a \approx 0.09$ fm and $a \approx 0.06$ fm.

PACS numbers: 12.38.Gc, 14.40.Pq

I. INTRODUCTION

Lattice calculations of the hyperfine splitting in charmonium usually ignore the contributions of the annihilation (disconnected) diagrams to both the vector J/ψ and the pseudoscalar η_c states. This simplification leads to an error, and our goal is to determine the actual value of the contributions. Perturbatively, the contribution of these diagrams in charmonium is expected to be small due to the OZI suppression, especially for the vector state [1]. However, nonperturbative effects, such as the $U_A(1)$ anomaly [2] and mixing with glueball and light hadronic states, might enhance it enough so that it becomes a nonnegligible fraction of the hyperfine splitting. Previous calculations [3, 4] using two-flavor gauge ensembles very roughly estimated the contribution to be within ± 20 MeV. They both confirm that there are significant difficulties in obtaining a signal for the disconnected diagrams due to noise, especially for heavy quarks.

In our work, the charm quarks are simulated with the clover fermion action with κ_c tuned to the physical charm quark mass. The disconnected diagrams are calculated stochastically with spin- and color-diluted sources. Our calculation improves on the previous ones in a number of ways. First, we use larger lattice volumes ($28^3 \times 96$, $48^3 \times 144$, and $40^3 \times 96$) and point-to-point (PTP) propagators, which significantly improves our statistics and signal-to-noise ratio. Point-to-point propagators reduce the relative standard error over time-slice-to-time-slice (TTT) propagators by one to three orders of magnitude. Second, our gauge ensembles have much finer lattice spacings a. We work with lattices with $a \approx 0.09$ fm (fine ensembles) and $a \approx 0.06$ fm (superfine ensemble). Table I gives the parameters of the ensembles. And lastly, we employ the unbiased subtraction technique [5] in the stochastic estimators used to determine the disconnected correlators. The success of this technique depends on the fast convergence of the hopping parameter expansion of the clover Dirac operator used in the subtraction. Considering that κ_c is still small for the charm quark at these lattice spacings, we use the terms of the expansion only up to third order in κ_c, which reduces the standard deviation of the disconnected correlator by an additional factor of about four.

In this study we attempt to determine the size of the effects of the disconnected diagrams on the mass of the η_c only. Our previous studies [6, 7] and our current work show that the effect of the charm annihilation on the vector state are much smaller than 1 MeV; thus we ignore it here and equate the hyperfine effects with the effects in the pseudoscalar only. Our calculations are done on two fully quenched and one dynamical ensemble with two light degenerate quarks and one strange quark (2+1 dynamical flavors) in the asqtad formulation [8]. In the fully quenched case, the

2

ensemble	a [fm]	m_l/m_s	volume	κ_c	# config.
QF	≈ 0.085	$\cdots$	$28^3 \times 96$	**0.120**, 0.127	410
QSF	≈ 0.063	$\cdots$	$48^3 \times 144$	**0.125**, 0.130	415
DF	≈ 0.086	0.0031/0.031	$40^3 \times 96$	**0.125**, 0.127	766

TABLE I: Run parameters of the quenched fine (QF), quenched superfine (QSF) and dynamical fine (DF) ensembles. The bold values of κ_c are the ones obtained by tuning the η_c mass and are used in this study. The nonbold κ_c values are from our previous studies [6, 7] and are listed for comparison.

disconnected η_c correlator can have at most additional contributions from the $U_A(1)$ anomaly and close-lying glueball states. In the 2+1 flavor dynamical case, the disconnected correlator can also couple to light hadronic states, which complicates the task at hand significantly. In both the 2+1 flavor dynamical and fully quenched cases we ignore contributions to the disconnected correlators from sea charm quark loops . To the extent that the disconnected contribution is small (first order), the sea charm quark effects are second order and so negligible at our level of precision. Our result that the contribution is indeed small makes the calculation self consistent.

This paper is organized as follows. Section II outlines the analytic framework in which we interpret our lattice data. Section III discusses some general properties of the disconnected propagators which follow from our analyses. In Section IV we give our fitting method for the disconnected propagator. Section V is dedicated to the specifics of the tuning of the charm quark mass. The final Section VI contains our results and conclusions.

II. GENERAL ANALYTIC FRAMEWORK

In this section we derive the shift of the mass of a flavor singlet state due to the contribution of the disconnected diagrams to its full propagator. Figure 1 shows the diagrammatic expansion of the full propagator, where with continuous lines we represent the charm quark propagators. The first term in this expansion is the connected piece and the rest are disconnected propagators containing charm quark loops. We denote the momentum-space connected propagator of a (pseudo)scalar meson as

$$C(p^2) = \frac{A}{p^2 + m_c^2}, \tag{1}$$

where A is a constant, and m_c is the "connected" mass of the meson. (The vector meson propagator has the same form as Eq (1), if we neglect the spin degrees of freedom). Then the full propagator is the infinite sum:

$$F(p^2) = \frac{A}{p^2 + m_c^2} + \frac{\sqrt{A}}{p^2 + m_c^2} \lambda(p^2) \frac{\sqrt{A}}{p^2 + m_c^2} + \frac{\sqrt{A}}{p^2 + m_c^2} \lambda(p^2) \frac{1}{p^2 + m_c^2} \lambda(p^2) \frac{\sqrt{A}}{p^2 + m_c^2} + \cdots, \quad (2)$$

where the first term is the connected piece $C(p^2)$ and the rest are terms which consist of disconnected quark loops of the same flavor as the meson's constituent quarks (see Fig. 1 for the diagrammatic representation of the three explicitly given terms). The function $\lambda(p^2)$ effectively describes all possible interactions between the quark loops in the disconnected pieces and the gauge fields, quarks of other flavors or effects such as the $U_A(1)$ anomaly, if relevant for the specific meson state. The disconnected propagator $D(p^2)$ is naturally the sum of all terms in Eq. (2), except the first one. After we sum the geometric progression in Eq. (2), we obtain:

$$F(p^2) = \frac{A}{p^2 + m_c^2 - \lambda(p^2)} = \frac{A}{p^2 + m_f^2}, \quad (3)$$

where m_f is the "full" meson mass we could calculate if we knew all terms that contribute to the full propagator. Thus, the difference between the mass that is usually computed from only the connected propagator and the actual mass is approximately [1]

$$\delta m = m_c - m_f \approx \frac{\lambda(-m_c^2)}{2m_c}. \quad (4)$$

In the last expression for simplicity we replaced the function $\lambda(p^2)$ with the value of its largest contribution in Eq. (2) at the pole $p^2 = -m_c^2$. Hence the sign of δm depends on the sign of $\lambda(-m_c^2)$. The mass shift δm due to the disconnected quark loops can be treated as a perturbation, in which case, to first order, both the connected and disconnected contributions can be computed without dynamical sea quarks of the constituent's flavor (heavy-quark-quenched case). In this case, only the first two terms in Eq. (2) survive and the disconnected propagator is reduced to the second term only (shown diagrammatically in Fig. 1, middle).

---

[1] The momentum dependence in $\lambda(p^2)$ leads to a first-order (in λ) renormalization of the connected pole residue, so there is a second order correction in our result that we safely ignore.
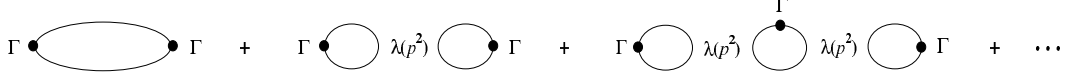
FIG. 1: Connected and disconnected diagrams contributing to the full propagator on lattices unquenched with respect to the charm quark.

III.   PROPERTIES OF THE DISCONNECTED PROPAGATOR

The asymptotic behavior at large times t of the full charmonium propagator, $F(t)$, is

$$F(t) = C(t) + D(t) = \sum_n \langle \Omega|O|n\rangle \langle n|O|\Omega\rangle e^{-E_n t} \xrightarrow[t\to\infty]{} \langle \Omega|O|0\rangle^2 e^{-E_0 t} , \qquad (5)$$

where the sum is over all eigenstates $|n\rangle$ of the Hamiltonian with corresponding energy eigenvalues E_n and $|\Omega\rangle$ is the vacuum state. In the last part of the above expression E_0 is the mass of the lightest state contributing to $F(t)$. The operator O is defined to be hermitian, in which case $F(t) \geq 0$ for all t. This is also true if we consider the PTP propagator $F(r)$ instead, where r is the Euclidian distance. The matrix defining the spin structure in the operator O is $\Gamma = i\gamma_5, i\gamma_i$ for the η_c and J/ψ states, respectively, in terms of Hermitian γ_5 and γ_i. At large distances r, the lightest possible modes that couple to the operator O should dominate in $F(r)$. The origin of these can be light glueballs and, in the dynamical case, the propagation of hadronic modes consisting of quarks lighter than the charm quark. Since $F(r)$ is nonnegative for all r, it follows that, when it dominates, $D(r)$ should also be nonnegative in the large distance limit. The sign of $D(r=0)$, with the above hermiticity condition on O, is strictly negative for the pseudoscalar (and positive for the vector). It follows that in the dynamical case, where $D(r)$ is dominant at large distances, $D(r)$ changes sign for the pseudoscalar. In the quenched case this sign flip occurs if there are glueballs lighter than the charmonium state studied. On the lattice, the TTT disconnected propagator is calculated as:

$$D(t) = c_\Gamma \langle L(0)^\star L(t)\rangle, \quad \text{where} \quad L(t) = \text{Tr}(\Gamma M^{-1}), \qquad (6)$$

and M is the charm quark matrix. The trace in $L(t)$ is over the Dirac, color and space indices. For the vector we have $\Gamma = i\gamma_i$, $c_\Gamma = 1$ and for the pseudoscalar $\Gamma = i\gamma_5$, $c_\Gamma = -1$. On the other hand, the PTP disconnected propagator is obtained in the following manner:

$$D(r) = \frac{c_\Gamma}{N_r} \sum_{r=|x-y|} \langle L(x)^\star L(y)\rangle, \qquad (7)$$
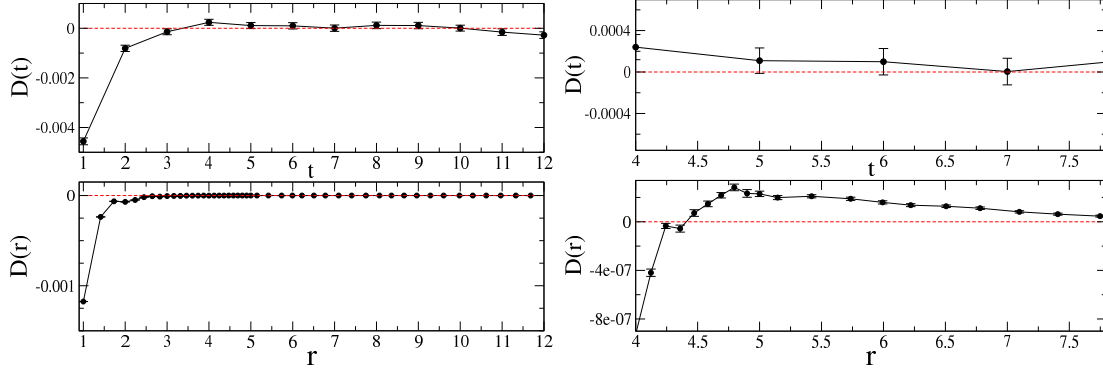
5

FIG. 2: Comparison of $D(t)$ and $D(r)$ for η_c for two different ranges of t and r. The results are from the calculation on the dynamical ensemble at $\kappa_c = 0.127$. The data for $D(r)$ was averaged in small bins in r for $r > 5$.

where x and y are lattice coordinates, the sum is over all pairs of lattice points at Euclidean distance $r = |x - y|$, N_r is the number of these pairs and there is a trace only over spins and colors in $L(x)$ (but not over space). From the previous studies [3, 4] it is known that the $D(t)$ signal disappears very quickly around $t = 2 - 3$. We work with the PTP disconnected propagator instead, since this way we benefit from both the additional data at noninteger distances and the much improved statistics. The correlator $D(r)$ has from one to three orders of magnitude smaller *relative* errors than the TTT disconnected propagator in the region where we have a signal. Figure 2 illustrates this statement by comparing $D(r)$ and $D(t)$ for η_c for two different ranges of r and t. Both propagators are calculated with $\kappa_c = 0.127$ on the dynamical lattices from Table I. In the right panel of Fig. 2, the comparison is done on a shorter range in order to emphasize the fact that we do have a clear signal for $D(r)$ in the range where the $D(t)$ signal is completely obscured by the noise. The result that the $D(r)$ signal is so much better than the one for $D(t)$ can be explained by the fact that in the calculation of $D(t)$ there are a great number of contributions from points, which although not far from each other in the t direction, are far in the 4d Euclidean space. For the disconnected correlator, the noise increases strongly with the distance and such points contribute nothing to $D(t)$ but noise. This problem is avoided when working with $D(r)$ instead. We also note that as predicted in the previous paragraphs, both $D(r)$ and $D(t)$ undergo a sign flip for the η_c state.

6

IV. FITTING THE DISCONNECTED PROPAGATORS

To determine δm for the η_c we use Eq. (4), which means that we have to obtain $\lambda(p^2)$ from our data for the PTP disconnected propagator. In order to fit our data for $D(r)$, we need a fitting model which satisfies the requirement that the charmonium disconnected propagator is treated as a composite object, which has contributions not only from the studied charmonium ground state, but also possible effects from excited charmonium states, states lighter than the charmonioum ground state and possibly the $U_A(1)$ anomaly. We also have to take into account that our data exhibits rotational symmetry violations at short distances, due to the finite lattice spacing.

To define such a fitting model it is easiest to start from the momentum space description of the disconnected propagator. A simplified form which describes its behavior in momentum space is

$$D(p^2) = \lambda(p^2) \left(\frac{\sqrt{A}}{p^2 + m_c^2} + \sum_{n=1}^{N} \frac{\sqrt{A^n}}{p^2 + (m_c^n)^2} \right)^2, \tag{8}$$

where we have included in the quark loops one ground state, characterized by mass m_c and N excited states with masses m_c^n (the index $n = 1, \ldots, N$). Here we also make the assumption that the interactions for all states are described by the same function $\lambda(p^2)$. In the fully quenched case, we model the function $\lambda(p^2)$ as

$$\lambda(p^2) = U + \frac{f}{p^2 + m_g^2}, \tag{9}$$

where U stands for possible effects of the $U_A(1)$ anomaly, so it is negative, and $f/(p^2 + m_g^2)$ is an effective light glueball term with m_g being the glueball mass. We assume that U, f, A and $A^{n=1\ldots N}$ change little for a wide range of momenta and will approximate them with constants in our model. In the 2+1 flavor dynamical case, the expression for $\lambda(p^2)$ could be more complicated. For example, we need to take into account the existence of both light glueballs and light hadronic modes in order to describe our data:

$$\lambda(p^2) = U + \frac{f}{p^2 + m_g^2} + \frac{l}{p^2 + m_l^2} + \cdots. \tag{10}$$

In the above l is a constant and m_l is the mass of one of the light hadronic modes. In practice we keep only one light hadronic mode in the above with an effective mass m_l that (we hope) describes well the long distance behavior of the PTP propagator.

We want to limit the number of free parameters in our model to as few as possible, since although our data is of much higher quality than in other studies, it is still difficult to resolve all of

the parameters in Eq. (8) from the disconnected propagator data. The masses m_c and $m_c^{n=1...N}$, for example, can be determined from fits to the TTT connected charmonium propagator $C(t)$, and then be used as constants in our fits. We obtain the ground state mass m_c with a very small fitting error, but the excited states masses $m_c^{n=1...N}$ are less well known. We can also determine with varing degrees of precision the constants A and $A^{n=1...N}$ from fits to $C(t)$, since they are proportional to the amplitudes of the ground and the excited states, respectively. We relate the PTP amplitude A to the corresponding TTT amplitude as follows: We Fourier transform the ground $C(p^2)$ propagator and then integrate over space:

$$\int d^3x \int \frac{d^4p}{(2\pi)^4} \frac{A}{p^2+m_c^2} e^{ipr} = \frac{A}{2m_c} e^{-m_c t}. \tag{11}$$

The RHS in the above is the TTT propagator, which implies a relation between the amplitude of the ground state in $C(t) = A_t e^{-m_c t} + \cdots$, denoted by A_t, and the factor A:

$$A = 2m_c A_t. \tag{12}$$

Another parameter that we can fix in our model using prior knowledge is the glueball mass m_g. We use the results for the lightest 0^{-+} glueball from Ref. [9], namely we set $m_g = 2563$ MeV, which is the value extrapolated to the continuum limit. We use this value for all of our lattice spacings, since in Ref. [9] it was found that the glueball mass does not vary much at fine lattice spacings and is compatible with the continuum extrapolated result. On the dynamical ensembles we have to take into account also the contribution of the light hadronic modes, and preferably we want also to set the mass m_l to an appropriate constant. In our previous work [6, 7] we found that the long distance behavior of the PTP pseudoscalar propagator on the dynamical ensemble can be fitted well with a light state of mass $am_l \sim 0.42$. This is very close to the physical mass of the η' of 958 MeV; thus we fix m_l to the mass of the η'. Although there are states lighter than the η' contributing as well (such as the η, multipion states *etc.*), this approximation is probably satisfactory, because the modes lighter than the η' would mix even less with the heavy η_c state, and we cannot distinguish their signal at our level of statistics. Thus the only free parameters in our model remain U, f and l (the last one is present only in the dynamical case).

The summary of our fitting strategy in the simpler fully quenched case is as follows:

- On a given lattice ensemble we calculate the TTT connected propagator of the η_c state. From fits to it with the asymptotic form $C(t) = A_t e^{-m_c t} + \sum_{n=1}^N A_t^n e^{-m_c^n t}$ we determine m_c, $m_c^{n=1...N}$, A_t and $A_t^{n=1...N}$. Using Eq. (12) with the substitution $m_c^{(n)} \rightarrow \sqrt{2(\cosh(m_c^{(n)}) - 1)}$

in order to take into account lattice discretization effects, we obtain A and $A^{n=1...N}$. We use the central values of all of the above parameters as constants in our model function Eq. (8).

- We also fix the parameter m_g in Eq. (9), using prior knowledge.

- In Eq. (8) we replace p^2 with $\sum_i 2(1 - \cos(p_i))$ and all the masses with the appropriate expression as done in the first item above for $m_c^{(n)}$, to account for the lattice discretization effects. Equation (8) can be rewritten in a form linear in the two parameters U and f, which is more convenient for fitting purposes:

$$D(p^2) = UT_1(p^2) + fT_2(p^2). \tag{13}$$

  Next, we do a discrete Fourier transformation of $T_{1,2}(p^2)$ on a lattice of an appropriate size and obtain the functions $T_{1,2}(r)$ at discrete values of r. We tabulate $T_{1,2}(r)$ at each distance $r \leq 15$. This range of r is sufficient, since our signal is too noisy for $r > 15$. Thus using the linear model

$$D_{\text{fit}}(r) = UT_1(r) + fT_2(r), \tag{14}$$

  we fit our data for the PTP disconnected charmonium propagator $D(r)$ in order to extract U and f.

- With the fit values of U and f at hand, we determine $\lambda(-m_c^2)$ and δm from Eqs. (4) and (9).

The fitting procedure in the 2+1 flavor dynamical case is quite similar. In addition there we fix appropriately the light mass m_l and use a fitting form with three tabulated terms:

$$D_{\text{fit}}(r) = UT_1(r) + fT_2(r) + lT_3(r). \tag{15}$$

After we extract the parameters U, f and l, we solve again for δm with the appropriate $\lambda(-m_c^2)$ from Eq. (10).

The error due to the assumption that the participating masses and the amplitudes A and $A^{n=1...N}$ in our model are constants is discussed in Sec. VI. The success of our fitting model depends on how well it approximates the interaction dynamics on the lattice and on the quality of our data. An essential part of the construction of the fitting model for the PTP disconnected propagator turned out to be the number of excited states N which we have to include. The excited states have larger contributions to the disconnected propagator at a given distance than they have in the case of the connected propagator. This means that a good knowledge of the spectrum of excited

9

states is required in order to fit the disconnected propagator. In the disconnected diagram with net propagation distance r the connected η_c propagates on average less than half the distance before annihilating and again less than half after reappearing. This means that a reliable fit to the connected propagator yields masses and amplitudes which we can use in fits to the disconnected propagator at least at twice the distance, where the signal may be too noisy. Thus we are limited to fits of the connected propagator with $t_{min} = 2$ or 3 and use the extracted parameters in the disconnected fits from $r_{min} = 4$ or 6.

To obtain the charmonium spectrum from the fits to the connected propagator, we employ a fitting model which forces the splittings between the states to be positive, essentially creating a "tower of states". The priors for the logarithms of all the splittings are the same (*i.e.*, we assume the states are equidistant as a first approximation) and so are their widths. We used a set of different values for the splitting priors and their widths to check the stability of the resulting spectrum. We found that the extracted masses were stable for a relatively wide range of priors. Our best fits have the splitting priors in the range of 570–770 MeV. Still, this approach is not intended to provide a reliable determination of the masses of excited quarkonium. Rather, we use this heuristic model to understand the role played by excited states in our result.

In our fitting model we also require (through the use of priors) that the amplitudes of the excited states are no larger than the ground state amplitude. Without this restriction, we noticed that the amplitudes of the excited states grow noticeably larger than that of the ground state (where we define this to mean difference larger than 1.5σ). The assumption that this should not happen stems from general considerations: The wave function at the origin is smaller for an excited state than the ground state, simply because the excited state wave function spreads out more. This is a characteristic of non-relativistic potential models. There is also some support from experiment: The decay constant of ψ' is smaller than that of the J/ψ (PDG values: 279(8) MeV *vs.* 411(7) MeV, respectively). Lattice studies of the light-light [10] and heavy-heavy [11] meson sectors also confirm this expectation. But other lattice calculations, such as in Ref. [12] for the heavy-light meson case, show the first excited state decay constant growing larger than the ground state one. A possible explanation for this discrepancy in the last study is that the contributions of the neglected higher excited states became lumped into the amplitude of the first excited state.

In our fitting model, the requirement that the amplitudes of the excited states do not grow much larger than the ground state amplitude, we hope, prevents the "clumping" of states with similar masses into an effective state with a large effective amplitude. However, since we use only a
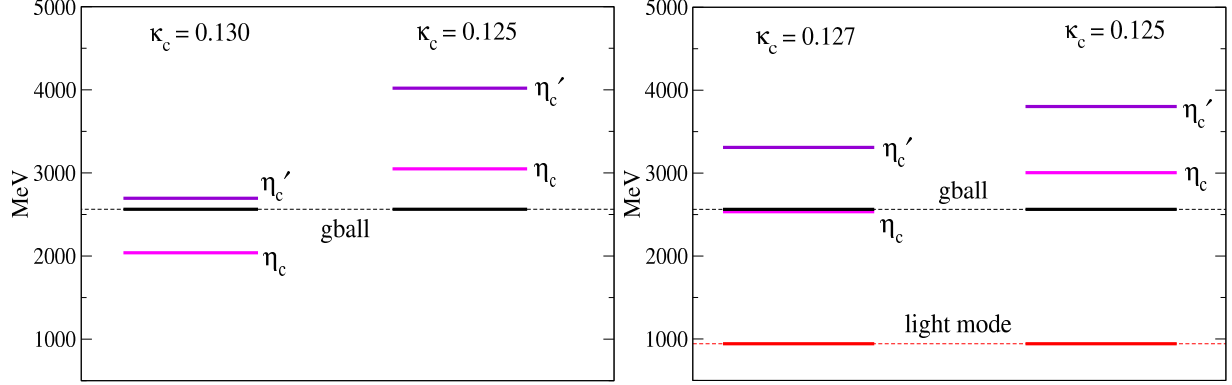
10

FIG. 3: (Left panel) Relative positions of the charmonium states with respect to the 0^{-+} glueball mass with $m_g = 2563$ MeV on the quenched superfine ensemble, for different k_c. (Right panel) Same for the dynamical ensemble.

Gaussian prior to constrain the logarithm of the excited state amplitudes, it still often happens, depending on the number of states included, that the highest state in the fit and sometimes the next highest end up with large amplitudes. We interpret this outcome as a clumping of multiple unresolved states of similar mass. How we count them affects our result for δm. To compensate for this effect we represent the resulting contribution as a sum of states of similar mass:

$$\frac{A^N}{(p^2 + (m_c^N)^2)} \approx \sum_{k=1}^{M} \frac{A'}{(p^2 + (m_c^N)^2)}.$$ (16)

where $M \approx A^N/A' \equiv A_t^N/A_t$ (the ratio of the highest excited state amplitude to the ground state one). Each of the states in the sum above should contribute $\sqrt{A^N/M}/(p^2 + (m_c^N)^2)$ in Eq. (8). Since there are M of them, the contribution of the effective N-th state in Eq. (8) is modified to $\sqrt{A^N M}/(p^2 + (m_c^N)^2)$. In effect, we multiply the amplitude A^N by the number M of its contributing states before using it in Eq. (8) in order to correctly account for the possibility that the N-th state is an effective one. Note that increasing the multiplicity in this way always decreases δm. Thus in our analysis of systematic effects, we explore the sensitivity of our result to this assumption.

V. TUNING THE CHARM QUARK MASS

As we already stated in the Introduction, we use clover fermions to generate the connected and disconnected charmonium propagators. This means that we have to tune the hopping parameter, κ_c, to correspond to the physical charm quark mass. In our preliminary work [6, 7] we tuned κ_c

11

using the kinetic mass of D_s *i.e.*, we used the Fermilab interpretation of the clover fermions. For the fully quenched ensembles this tuning was rather approximate. In this work we adopt a different approach, namely, we tune κ_c by matching the rest mass of the η_c to its physical mass instead with an accuracy of several percent. Our current approach is more appropriate for the purposes of determining δm, since it positions the charmonium η_c state correctly with respect to the lightest glueball with which it might mix. This is important, because, depending on whether the mass of the charmonium state is heavier or lighter than the lightest glueball, δm might change in absolute value or even undergo a sign flip. Figure 3 illustrates this statement by showing the masses of the η_c, η_c' and the lightest 0^{-+} glueball on the superfine quenched (left) and the dynamical fine ensembles (right), for values of κ_c obtained by our previous and current tuning methods. In the quenched superfine case, for example, using the value $\kappa_c = 0.130$ from the kinetic mass tuning of D_s, gives a rest mass of the η_c lighter than its physical value and lighter than the lightest glueball. This implies that their mixing will "push" the η_c mass to lower values on the lattice. However, if the η_c rest mass assumes its correct physical value (achieved at $\kappa_c = 0.125$), the effect of the glueball mixing would be exactly the opposite. We conclude that although the kinetic mass κ_c tuning is the correct method in cases when we want to determine various mass spectrum splittings in the charmonium system, for our study the appropriate method is to tune the charm quark mass using the rest mass of the charmonium state we are interested in. (An alternative method which could render both the charmonium splittings and the rest masses correct, is to have different values for the spatial and temporal hopping parameters, a strategy which we do not employ here.)

VI. RESULTS AND CONCLUSIONS

In this section we present our results for the mass shift δm due to the contribution of the disconnected diagrams for the η_c on all of the ensembles from Table I. We use 72 Z_2 random sources per lattice with spin and color dilution to compute the disconnected propagators on all of our ensembles (which means there are 72×12 quark matrix inversions per lattice performed). To explore the systematic effects which arise in the determination of δm due to our incomplete knowledge of the charmonium spectrum, we studied in more detail the data from the quenched fine ensemble. We fitted the connected propagator using 4, 5, 6, and 7 states and used the extracted masses and amplitudes to fit the disconnected propagator $D_{\eta_c}(r)$, as described in Sec. IV, in each case.

Table II shows the results from the fits to the connected propagator in its upper and middle

#states	m_{η_c}	m_c^1	m_c^2	m_c^3	m_c^4	m_c^5	m_c^6	χ^2/DOF
4	1.3708(2)	1.67(3)	1.98(6)	2.59(5)	$\cdots$	$\cdots$	$\cdots$	1.6
5	1.3708(2)	1.68(3)	1.98(7)	2.56(5)	2.81(13)	$\cdots$	$\cdots$	1.6
6	1.3708(2)	1.67(3)	1.94(6)	2.16(9)	2.42(10)	2.67(11)	$\cdots$	1.4
7	1.3709(2)	1.67(3)	1.93(7)	2.13(8)	2.34(9)	2.54(9)	2.74(9)	1.3

#states	A_t	A_t^1	A_t^2	A_t^3	A_t^4	A_t^5	A_t^6
4	0.589(3)	0.58(19)	1.63(34)	5.64(31)	$\cdots$	$\cdots$	$\cdots$
5	0.589(3)	0.59(19)	1.58(35)	4.81(45)	0.91(36)	$\cdots$	$\cdots$
6	0.589(3)	0.56(18)	1.06(33)	0.93(35)	0.86(34)	4.55(50)	$\cdots$
7	0.588(3)	0.56(17)	0.90(31)	0.95(35)	0.95(37)	0.97(38)	3.74(60)

#states	δm [MeV]	δm^{corr} [MeV]
4	-3.61(24)	-1.59(15)
5	-3.31(29)	-1.62(15)
6	-2.74(24)	-1.75(20)
7	-2.45(22)	-1.88(18)

TABLE II: Masses (top) and amplitudes (middle) in lattice units extracted from fits to the connected propagator on the QF ensemble with different numbers of states (4, 5, 6, and 7). The lowest part of the table shows the mass shift δm, calculated using the results from the upper two parts of the table. Also shown is the "corrected" mass shift δm^{corr}, which is obtained using the systematic error estimation method described at the end of Sec. IV.

subtables. All of the fits were performed on the same time range ($t = 2 - 45$). We see that the χ^2/DOF improves with adding more states to the fitting model and the amplitudes of the excited states become smaller at the same time. The extracted masses of the ground and the two lowest excited states appear to be quite independent of the number of states included in the fit. The third and higher excited states on the other hand do depend on the number of states. This is not very surprising; these states are much more difficult to extract and are likely to be effective states. Their amplitudes also are more likely to grow large, lending support to this interpretation.

ensemble	m_{η_c}	m_c^1	m_c^2	m_c^3	m_c^4	m_c^5	m_c^6	m_c^7	m_c^8
QF	1.3708(2)	1.67(3)	1.94(7)	2.16(9)	2.42(10)	2.67(11)	$\cdots$	$\cdots$	$\cdots$
QSF	0.9734(2)	1.22(2)	1.41(7)	1.63(9)	1.87(10)	2.10(10)	$\cdots$	$\cdots$	$\cdots$
DF	1.2749(4)	1.58(3)	1.88(7)	2.08(9)	2.26(8)	2.43(8)	2.62(10)	2.83(11)	3.05(12)

ensemble	A_t	A_t^1	A_t^2	A_t^3	A_t^4	A_t^5	A_t^6	A_t^7	A_t^8
QF	0.589(3)	0.56(18)	1.06(33)	0.93(35)	0.86(34)	4.55(50)	$\cdots$	$\cdots$	$\cdots$
QSF	0.270(2)	0.32(10)	0.39(13)	0.33(13)	0.33(13)	4.44(24)	$\cdots$	$\cdots$	$\cdots$
DF	0.822(7)	0.84(21)	1.00(37)	1.30(47)	1.40(49)	1.30(47)	1.17(43)	1.07(40)	0.98(38)

TABLE III: Parameters extracted from fits to the TTT connected η_c propagator $C(t)$ for each ensemble. Masses and amplitudes are in lattice units. The χ^2/DOF for the fits is 1.4, 2.2, and 1.4 for the QF, QSF, and DF ensembles, respectively. The $t_{\min}$ for these fits is 2, 3, and 2. The central values of the masses and amplitudes are used as constants in the fitting model for the disconnected η_c propagator.

The effect of the number of states in each fit on δm is shown in the lower part of Table II. We also show there the corrected value of the mass shift δm^{corr}, which is obtained by modifying the amplitudes that are significantly larger than the ground state one (*i.e.*, the amplitudes of the second and third excited states for the 4- and 5-state fits and the highest excited state one in the case of 6- and 7-state fits), in the manner described at the end of Sec. IV. The difference between δm and δm^{corr} gives some idea of the systematic error. This systematic error grows when there are fewer states in the fitting model, possibly because the charmonium spectrum is not well represented by it over the fitting range. This effect is also signaled by a growing χ^2/DOF in these cases. It is encouraging that δm^{corr} is very consistent between the different fits.

Among these results for δm, the one we consider best is the one obtained using the 6-state fit to the connected propagator, for two reasons. First, this is the fit with the fewest excited states to achieve χ^2/DOF below 1.5, a value we consider to be on the boundary between "good" and "bad" fits. Second, the excited state spectrum is close to the picture where all amplitudes but that of the highest included state are not much larger than the ground state amplitude. We expect the highest excited state to reflect the fact that we work with finite number of states in the fitting model, and thus likely to have a large effective amplitude.

We apply the same criteria when we repeat the whole calculation on the rest of the ensembles

in this study. We adopt the results for δm from the best of our fits as the final answer and report the difference between δm and δm^{corr} as an asymmetric systematic error. Results for all three ensembles are summarized in Table III. The number of states in the preferred fit is chosen according to the criteria described above, resulting in six states for the quenched ensembles and nine for the dynamical one. For the quenched superfine ensemble however we did not obtain a good χ^2/DOF for $t_{\min} = 2$ or 3, even when we included more than six states.

To complete our results for each ensemble, we fit our $D_{\eta_c}(r)$ data, as described in Section IV, with the values for the model parameters taken from Table III, respectively. The glueball mass in our model is the constant $m_g = 2563$ MeV, and in the dynamical case we also fix $m_l = 958$ MeV. Figures 4 (both panels) and 5 (left panel) show our results for the η_c disconnected propagator for each of the studied ensembles and the best fits to the data. In Table IV we give the fitting parameters, ranges, χ^2 per degree of freedom and our final result for the mass shift δm for each ensemble.

All of our results consistently show $\delta m < 0$ (meaning an increase on the η_c mass). It is notable that this is opposite the prediction of perturbation theory [14]. Even without a quantative calculation of the mass shift δm one might expect that it will be negative. First, according to the mixing models [13], if the $U_A(1)$ anomaly has an effect on the η_c, it should make its mass larger. In our model this is reflected in the fact that we obtain $U < 0$. Second, the light glueball happens to be lighter than the η_c, and when they mix, similarly, the mass of the η_c is pushed up. This is reflected in our finding that $f/(-m_c^2 + m_g^2) < 0$. The same is valid for the effect of light hadronic modes on m_f in the dynamical case. The mass shift itself is similar for the two quenched ensembles: $\delta m = -2.74(24)$ and $-2.18(47)$ MeV for the fine and the superfine one, respectively, where the errors are statistical only. We estimate the systematic effects stemming from our limited knowledge of the charmonium excited states as described in Sec. IV, to be around 1 MeV, applied in the direction of decreasing the absolute value. This estimate is based on the difference between the above values for δm and their corresponding δm^{corr}, the latter being $-1.75(20)$ MeV and $-1.15(28)$ MeV, respectively. The quenching of the light quarks is, of course, another source of systematic error which might not be negligible.

The dynamical ensemble yields a larger value for the η_c mass shift: $\delta m = -8.52(24)$ MeV (the error is statistical only). We did not determine the systematic effects of the excited states (through δm^{corr}) in this case, because the amplitudes of the excited states in the connected propagator did not grow much larger than the ground state one (*i.e*, they differ less than 1.5σ). This is not too

surprising considering that we already use 8 excited states in our fit to the connected propagator in order to achieve a good χ^2/DOF. The discrepancy in the determined values of δm in the quenched and the dynamical cases is most likely due to much larger systematic errors (other than the excited states contribution) in the latter case. For example, our simplified model does not account for the complications due to the mixing with the open charm threshold. Above this threshold there are numerous close-lying open-charm states. These discretized (in finite volume) continuum states do not fit the tower-of-states model: At our lattice size their level spacing is approximately ten times smaller than the typical level spacing in our tower-of-states model, and they have a degeneracy that grows rapidly with S-wave phase space. Further, their amplitudes are likely to be much smaller than the amplitudes of the "bound" states. They would appear as clumped, effective states in the tower-of-states model. To the extent they are important in our analysis, correcting for their clumping would tend to reduce the absolute value of δm.

In Table IV we also present separately the contribution of the anomaly δm_U to the total mass shift for each of the ensembles. The values of δm_U are roughly the same as the one predicted in Ref. [13] using mixing models. Our numerical results show that the contributions in MeV of the $U_A(1)$ anomaly is about half to 2/3 of the final value. The effect of mixing of the η_c with light hadronic modes in the dynamical case is much smaller than 1 MeV and is practically negligible. This is not unexpected considering the large mass difference between them. Figure 5 (right panel) shows the values of δm for each ensemble.

In addition to the statistical error in these values, another source of uncertainty in δm is the κ_c tuning. We have negligible κ_c-tuning errors for the superfine quenched (and the dynamical) case where the tuning is done to $1 - 2$ %, but the η_c mass in the case of the quenched fine ensemble is about 7% heavier than the physical one. This leads to an asymmetric correction to the δm in the case of the quenched fine ensemble by about 1 MeV in the direction of increasing its absolute value. We obtained this correction by assuming that the parameters U and f change negligibly for small mass fluctuations and there is only an explicit dependence on m_c in Eq. (4). Then we equate the systematic error with the difference in δm when we use the physical and the measured value of the mass of the η_c.

Finally, the last source of uncertainty in δm originates from the assumption that the masses and amplitudes in the fitting model Eq. (8) are constant, when in reality we know them up to their statistical errors. We estimate the effect of this assumption by varying these masses and the amplitudes within their statistical errors when fitting the disconnected propagator and recalculating δm.

16

We found that the resulting error for the quenched ensembles is within the statistical uncertainty and we neglect it in the final error budget for these ensembles. For the dynamical ensemble this error turned out to be 2 MeV. In this case we add it to the statistical error for this ensemble in Fig. 5 (right panel).

We mentioned in the Introduction that we equate the effects of the disconnected diagrams on the hyperfine splitting in charmonium with the mass shift they induce in the η_c only. In other words, we ignore the possible mass shift they cause in the J/ψ. We base this approximation on our attempt to estimate the effect on the vector using a fitting procedure similar to the one we used for the η_c. Our data for the vector is more noisy and the signal in the PTP propagator dies out at shorter distances than in the pseudoscalar case, due to the larger mass of the J/ψ. We found the effects of the disconnected diagrams for the vector is much smaller than 1 MeV and thus, they are within the statistical error of δm for η_c.

In conclusion, based on our results for the mass shift in η_c in the quenched case, the charmonium hyperfine splitting is decreased by $1 - 4$ MeV when we take into account the disconnected diagrams. This range is represented visually by the band between the slashed blue lines in Fig. 5 (right panel). In this final range for δm we ignore the dynamical result on the basis of its much larger and much less reliably estimated systematic effects, which require further study.
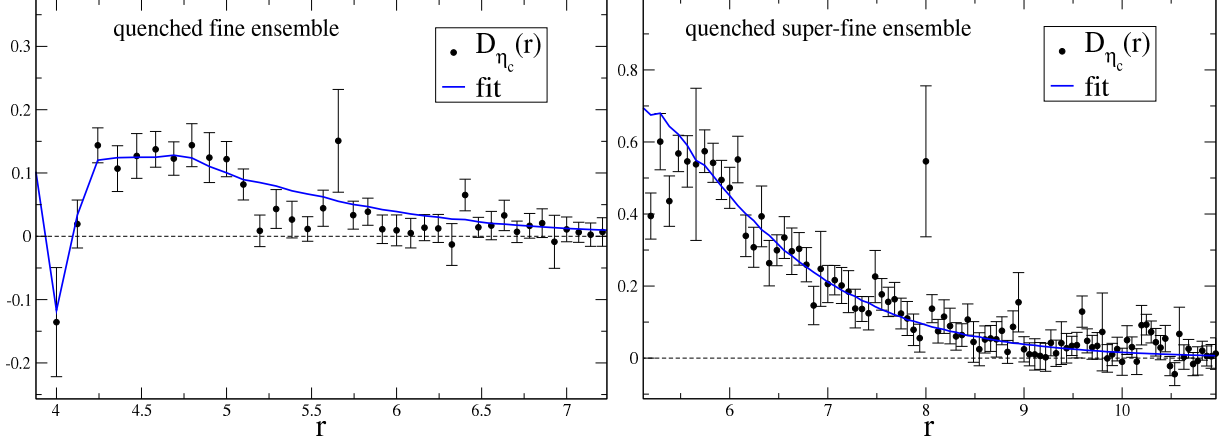
FIG. 4: (Left panel) The η_c disconnected propagator *vs.* the Euclidean distance r in lattice units for the quenched fine ensemble at $\kappa_c = 0.120$. Fluctuations in the data larger than the statistical errors are due to rotational symmetry violations.[a] (Right panel) Same for the superfine quenched ensemble at $\kappa_c = 0.125$.

[a]A Fourier transform of a monotonic function performed on a discrete lattice (which violates rotational symmetry) may exhibit non-monotonic "fluctuations".
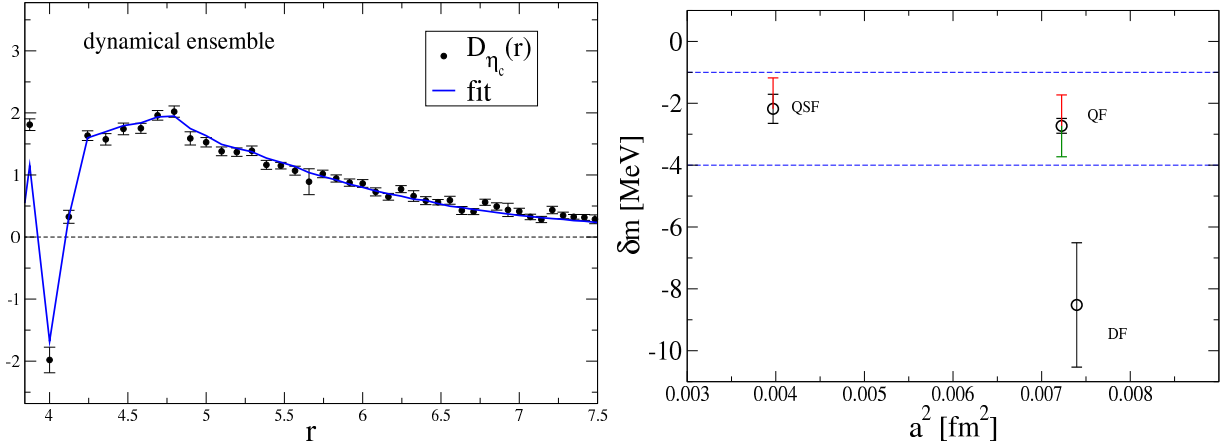

FIG. 5: (Left panel) The η_c disconnected propagator *vs.* the Euclidean distance r in lattice units for the dynamical fine ensemble at $\kappa_c = 0.125$. (Right panel) The mass shift δm for the quenched fine (QF), quenched superfine (QSF), and dynamical fine (DF) ensemble. The black error bars denote the statistical errors for the QF and QSF results. For the DF ensemble, the black error bar also includes the error due to specific assumptions in the fitting model as described in the text. The asymmetric red error bar originates from the systematic error due to our incomplete knowledge of the excited charmonium spectrum. The asymmetric green error bar is due to the κ_c mistuning in the QF case. The band between the two slashed blue lines encompasses the most likely range of δm based on the quenched data.

18

ensemble	$U \times 10^3$	$f \times 10^3$	$l \times 10^4$	δm [MeV]	δm_U [MeV]	$r_{\min} - r_{\max}$	χ^2/DOF
QF	$-2.31(36)$	$1.00(14)$	$\cdots$	$-2.74(24)^{+1.0}_{-1.0}$	$-1.81(28)$	$4 - 7$	$36/32$
QSF	$-6.53(35)$	$0.240(65)$	$\cdots$	$-2.18(47)^{+1.0}_{-0}$	$-1.01(53)$	$6 - 10$	$60/63$
DF	$-5.29(41)$	$2.28(15)$	$0.413(52)$	$-8.52(24)^{+2.0}_{-2.0}$	$-4.45(21)$	$4 - 10$	$111/82$

TABLE IV: Fitting results for the disconnected η_c propagators for each ensemble. The parameters U, f and l are in lattice units. The total mass shift is δm as defined in the text; the first error on the values is statistical, the second originates from various systematic effects as explained in the last section. The mass shift due exclusively to the effects of the anomaly is δm_U.

[1] S. Okubo, Phys. Lett., **5** (1963) 165. G. Zweig, CERN report TH-412 (unpublished); J. Mandula, J. Weyers and G. Zweig, Ann. Rev. Nucl. Sci., **20** (1970) 289; J. Iizuka, Prog. Theor. Phys. Suppl., 37-38, **21** (1966).

[2] G. 't Hooft, Phys. Rev. Lett. **37** (1976); T. Schäfer and E. V. Shuryak, Rev. Mod. Phys. **70** (1998) 323.

[3] C. McNeile and C. Michael, Phys. Rev. **D70** (2004) 034506 [hep-lat/0402012].

[4] P. de Forcrand *et al.* [QCD-TARO Collaboration], JHEP 0408 (2004) 004 [hep-lat/0404016].

[5] C. Thron *et al.*, Phys. Rev. **D57**, 1642 (1998).

[6] C. DeTar and L. Levkova, PoS(LAT2007) 116 [arXiv:0710.1322]

[7] L. Levkova and C. DeTar, PoS(LAT2008) 133 [arXiv:0809.5086]

[8] K. Orginos and D. Toussaint (MILC), Phys. Rev. **D59**, 014501 (1999) [hep-lat/9805009]; D. Toussaint and K. Orginos (MILC), Nucl. Phys. Proc. Suppl. **73**, 909 (1999) [hep-lat/9809148]; G. P. Lepage, Phys. Rev. **D59**, 074502 (1999) [hep-lat/9809157]. J. F. Lagäe and D. K. Sinclair, Phys. Rev. **D59**, 014511 (1999) [hep-lat/9806014]. K. Orginos, R. Sugar, and D. Toussaint, Nucl. Phys. Proc. Suppl. **83**, 878 (2000) [hep-lat/9909087].

[9] Y. Chen *et al.*, Phys. Rev. **D73:014516** (2006) [hep-lat/0510074].

[10] C. McNeile and C. Michael [UKQCD Collaboration], Phys. Lett. **B 642**, 244 (2006).

[11] J. J. Dudek, R. G. Edwards, and D. G. Richards, Phys. Rev. **D73:074507** (2006).

[12] T. Burch *et al.*, Phys. Rev. **D79:014504** (2009) [arXiv:0809.1103].

[13] T. Feldmann, P. Kroll and B. Stech, Phys. Rev. **D58:114006** (1998) [hep-ph/9802409].

[14] E. Follana *et al.*, Phys. Rev. **D75:054502** (2007) [0610092].